Published in Computers & Geosciences, 25, issue 8, 877-885, 1999
which should be used for any reference to this work

Multi-scale analysis of shell growth increments using wavelet transform ☆

M. Toubin [a,c], C. Dumont [a,c], E.P. Verrecchia [b,*], O. Laligant [a], A. Diou [a], F. Truchetet [a], M.A. Abidi [c]

[a] *Université de Bourgogne, Institut Universitaire de Technologie, Le2i, 12 rue de la fonderie, 71200 Le Creusot, France*
[b] *UMR CNRS 5561 Biogéosciences, Université de Bourgogne, 6 bvd Gabriel, 21000 Dijon, France.*
[c] *IRIS Laboratory, Electrical Engineering Department, University of Tennessee, Ferris Hall, Knoxville, TN 37996-2100, USA*

Abstract

Shell increments contain information related to the evolution of the environment in which the organism grew during its biomineralization. To extract the information from variations in shell topography, a new and promising technique is presented, involving multi-scale analysis of the shell topography using a B-spline wavelet transform. An accurate non-contact optical system, based on laser triangulation, is used to map the shell surface. The resulting range image is treated as a grey-level image by using a multi-resolution approach based on the generalization of the cascade algorithm. This method allows reconstruction of non-subsampled images that correspond to the projection onto the space of the chosen scale of detail. This new approach provides an efficient tool for analyzing multi-scale information contained in growth increment rings and/or within quasi-periodic features. In conclusion, this approach can be applied to any 3D object, in order to extract features such as rhythmic information, color variations or object envelope.

Keywords: Range image; Multi-scale analysis; B-Spline; Cycles; Mollusks

1. Introduction

Many shells exhibit external growth ridges, called increments, which are used in paleontology to reconstruct the annual growth rate of present-day or fossil organisms. Under the microscope, bivalve shells have fine striations or growth lines resulting from mineralization, which can be interpreted as growth increments. Rosenberg (1975) defines an increment as a period of time "represented between the beginning of a unit of structure or composition, and the beginning of the next adjacent unit". A growth line is characterized by an accumulation of $CaCO_3$, which can be described by its width and its relative thickness. The information included in the shell microtopography (the repetition of growth lines) can be different from the compositional factors, such as repetitive chemical composition. In this study, only the topographical aspect of the growth lines is taken into account. The amount of $CaCO_3$ deposition in each layer is frequently related to the secretion rate and biological clocks of organisms. A second type of control can influence the precipi-

☆ Code available at http://www.iamg.org/CGEditor/index.htm

* Corresponding author. Tel.: +33-3-8039-6356; fax: +33-3-8039-6356.
E-mail address: eric.verrecchia@u-bourgogne.fr (E.P. Verrecchia)

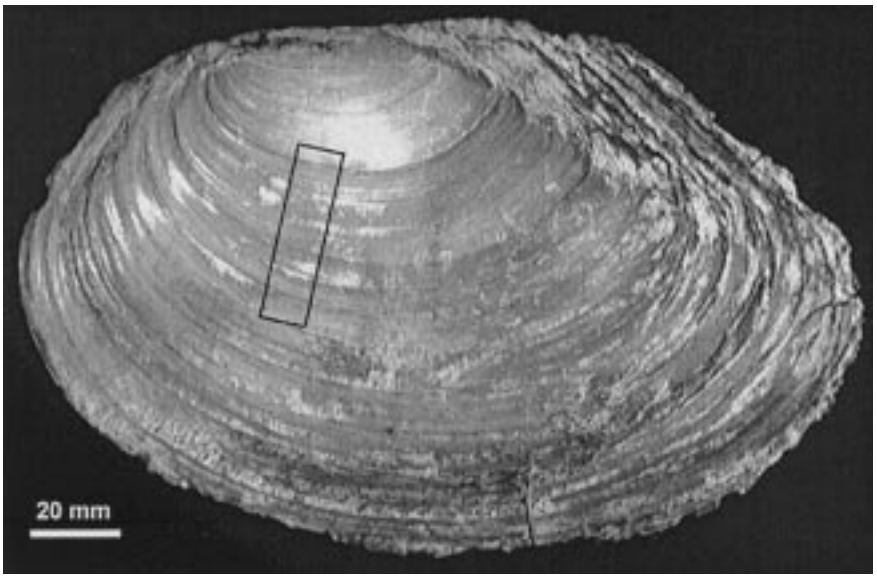

Fig. 1. General view of *Anadonta cygneae* (L.). This present-day bivalve shows numerous growth increments on its shell surface. Thickest rings correspond to winter growth.

tation rate: the effects of environmental factors (Rosenberg, 1975), i.e. temperature, photoperiods and tides, and the chemical composition of environmental fluids (Wada and Fujinuki, 1976). For example, in *Anadonta cygneae* (L.), the thicker ridges are related to winter growth. There are no more than ten of these thick layers, indicating a life expectancy of 10 years for this type of mollusk. In conclusion, two types of information are provided by the shell structure: (1) internal factors (i.e. growth rates and time periodicity) and (2) external factors (i.e. variations in the biogeochemical conditions of environments). The search for these two types of information inside accretionary shells of living or fossil organisms is critical for geologists who try to characterize the changes in the earth and organisms through time.

Previous studies of growth increments (Rhoads and Pannella, 1970) used thin sections of shell and acetate peel replicas of polished and acid-etched shell sections. The measurements of growth increments were performed either: (1) manually by counting growth rings with a microscope (Laurin and Gaspard, 1987); (2) using a profile pattern of grey levels obtained with a scanning electron microscope (Koike, 1980) or (3) using an optical transmission microdensitometer (Dolman, 1975) coupled with a digitizing micrometer eyepiece. Using these methods, the data obtained are related to the gap width between two increments, but do not take into account the amount of calcium carbonate deposited, i.e. the amplitude between the crest and trough separating two increments. Growth increments are usually counted in linear units. The distinction between generations (1st, 2nd and 3rd order) is made using the difference between the relative increment amplitudes. In addition, a spectral approach of growth records in invertebrates has been tried (Dolman, 1975) using a Fourier transform. This method, based on power spectra analysis, emphasizes the multiple periodicity of growth increments, which can be semi-annual, monthly or biweekly. However, this method does not provide the position or the harmonic amplitude value at each point. In contrast, the results given in this paper show that the wavelet transform keeps all the information (position, frequency and scale) and constitutes a powerful tool to investigate sequential data at various scales of resolution. As an example, the wavelet transform is used here to rank shell growth increments of a freshwater clam, *Anadonta cygneae* (L.) (Fig. 1).

The shell *Anadonta cygneae* (L.) is composed of calcite. Its mineralizing system involves five layers (Wilbur and Salenddin, 1983) in which mineral ions and organic molecules are exchanged, forming striations. To determine the influence of the environment on the growth rate, part of the *Anadonta cygneae* (L.) shell topography has been digitalized using a 3D laser scanning system. The information extracted is typically multiscalar, i.e. the 3D surface has low-scale and high-scale geometrical variations due to growth increments related to variations in climatic and environmental conditions and secretion rates. The extraction method proposed in this paper is based on the orthonormal wavelet analysis with cubic B-spline bases, which has the advantage of providing high interscale decorrela-

Fig. 2. Range image of *Anadonta cygneae* (L.) surface. Four cm^2 surface (4×1 cm) of shell has been digitized using 3D scanner (REPLICA 500). This surface covers at least two winter crests.

tion and, thus, can handle specific multiscale features of the shell.

After a description of the range image acquisition system, the multiresolution analysis is presented. The use of a cascade algorithm allows reconstruction of detailed and approximate images at various scales, without subsampling the image. Finally, the results are illustrated by images of *Anadonta cygneae* (L.), whose growth increments are recorded at various scales.

2. Range image acquisition

Part of the 3D topography of the *Anadonta cygneae* (L.) shell has been acquired using a non-contact optical sensor (3D scanners Ltd., 1995) based on laser triangulation (Fu et al., 1987) in order to determine the depth of the target points (Jarvis, 1983; Clark et al., 1995). A sheet of laser light is projected onto the shell surface. The resulting 3D curve, a stripe, is observed through two calibrated CCD cameras and the 3D position of the stripe points are computed by triangulation. The two cameras are set so that the image of the stripe intersects each image row (or column) at one place and the range information can be linked directly to one image coordinate. The sensor system is placed on a three axis translation stage, allowing the sensor to be moved along x, y and z axes. The object to be measured is placed on a table and is scanned by the sensor. At each step, the CCD cameras acquire two images of the stripe projected onto the object surface being scanned and the system computes the resulting depth information. The moving system has a positional accuracy of 50 μm and the optical measuring system also has an accuracy of 50 μm, which is enough to record every single shell growth increment. The distance between two increment edges has been checked under a scanning electron microscope after organic matter etching with sodium hypochlorite and gold coating.

Spatial sampling resolution is set in order to obtain the best correspondence between the scale grid imposed by the use of a dyadic algorithm and the amount of detail expected at each scale. Digitization of the shell topography results in a range image. Fig. 2 shows an example of a range image corresponding to the 1×4 cm scanned area of a shell. The depth infor-

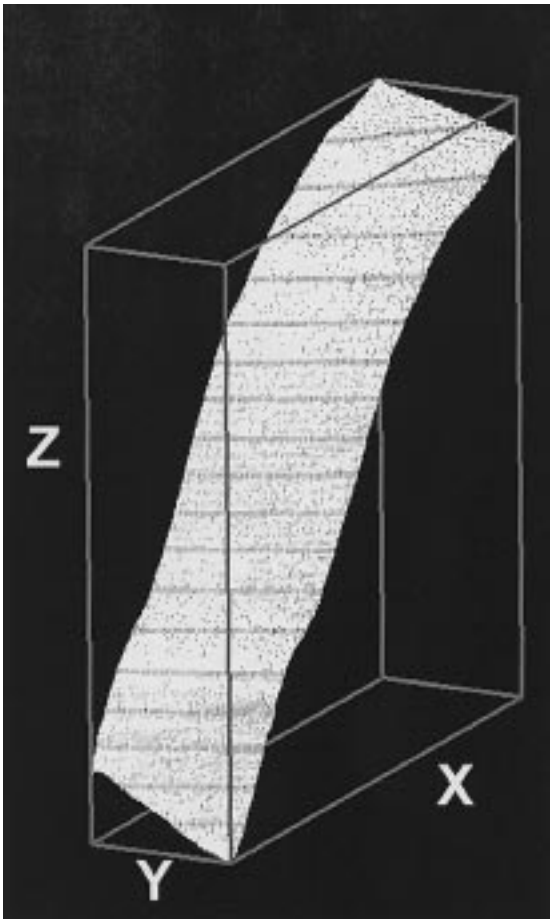

Fig. 3. 3D view of one part of shell that has been digitized (width = 25.6 mm, length = 6.4 mm, height = 15.4 mm). Position of (x, y, z) coordinate system.

mation in range images is grey level coded and the range image is interpreted as a 2D image (Garcia et al., 1998). Range images can also be viewed as 3D surfaces using a quad-mesh representation (Fig. 3), because the (x, y, z) coordinates relative to each pixel composing range images can be computed.

3. Multiresolution analysis: projection on orthogonal subspaces

The multiresolution orthogonal scheme used in this study has been defined by Meyer (1990) and Mallat (1989a). A function of L^2 (the continuous signal being analyzed) is orthogonally projected on a series of embedded closed subspaces V_j with $V_j \subset V_{j-1}$. The orthogonal complement of V_j in V_{j-1} is W_j with $V_{j-1} = V_j \oplus W_j$ and there exists an orthogonal basis for these subspaces (the orthogonal wavelet basis). This multiresolution analysis is dyadic if $f(x) \in V_j \Longrightarrow f(2x) \in V_{j-1}$.

Let a_n^j be the coefficient of the approximate function and d_n^j the wavelet coefficients for the j-resolution. The projections on the two bases (subspaces V_j and W_j) are:

$$\begin{aligned} a_n^j &= \langle f,\ \varphi_{j,n}\rangle \\ d_n^j &= \langle f,\ \psi_{j,n}\rangle \end{aligned} \tag{1}$$

where φ is the scale mother function and ψ is the wavelet mother function, with:

$$\varphi_{j,n}(x) = 2^{-j/2}\varphi(2^{-j}x - n). \tag{2}$$

Mallat (1989b) showed that the projection on each class leads to a convolution operation with an unique filter. The following relations are obtained on two suiting levels of resolution ($j-1$ down to j):

$$a_n^j = \sum_k \tilde{h}(2n-k)a_k^{j-1} \tag{3}$$

where $\tilde{h}(k) = h(-k)$ and $h(k) = \langle \varphi,\ \varphi_{-1,k}\rangle$

$$d_n^j = \sum_k \tilde{g}(2n-k)a_k^{j-1} \tag{4}$$

where $\tilde{g}(k) = g(-k)$ and $g(k) = \langle \psi,\ \varphi_{-1,k}\rangle$

h being the scale function filter and g the wavelet function filter. Direct computation of these projections, respectively, on V_j and W_j, consists of evaluating:

$$A_j f = \sum_{n=-\infty}^{+\infty} a_n^j \varphi_{j,n} \tag{5}$$

$$D_j f = \sum_{n=-\infty}^{+\infty} d_n^j \psi_{j,n}. \tag{6}$$

A new algorithm has been developed allowing the construction of the zero-scale approximation. It is characterized by its coefficients a_n^0 of the signal projection onto any sub-spaces V_j or W_j with $j > 0$. Since the origin of the scale is chosen arbitrarily, the accuracy of the approximation can be freely defined. The coefficients a_n^0 represent the 'coordinates' of $A_0(A_j f)$ or $A_0(D_j f)$, in the first case $a_n^0 = \langle A_j f, \varphi_{0,n}\rangle$ and in the second case $a_n^0 = \langle D_j f, \varphi_{0,n}\rangle$. If $j > 0$, the zero scale approximation of $A_j f$ is obtained by:

$$A_0(A_j f\ ) = A_1(A_j f\ ) + D_1(A_j f\ ). \tag{7}$$

If $W_1 \perp V_1$ and $V_j \subset V_1$, then $W_1 \perp V_j$, therefore $D_1(A_j f) = 0$, which leads to:

$$A_0(A_j f\ ) = A_1(A_j f\ ). \tag{8}$$

The generalization of the previous equation allows the formulation of:

$$A_0(A_j f\ ) = A_j(A_j). \tag{9}$$

The operator A_j is idempotent, therefore, the final equation is:

$$A_0(A_j f\ ) = A_j f. \tag{10}$$

Since the transform of the signal decomposition is bijective, the coefficients $A_0(A_j f)$ are given by the reconstruction of a_n^j obtained with the signal analysis of f and with all the detail coefficients deleted for each level j. These coefficients will form an approximation at the zero-scale of the projection of f on the subspaces V_j.

The following equation is used to compute the approximation of the detail signal f at level 0:

$$A_0(D_j f\ ) = A_1(D_j f\ ) + D_1(D_j f\ ). \tag{11}$$

If $W_i \perp W_j$ and $\forall j \neq 1,\ A_0(D_j f\ ) = A_1(D_j f\ )$. Continued decomposition yields:

$$A_0(D_j f\ ) = A_j(D_j f\ ) + D_j(D_j f\ ). \tag{12}$$

Because $V_j \perp W_j$ and the operator D_j is idempotent:

$$A_0(D_j f\ ) = D_j f \tag{13}$$

Reconstruction of details at level j is performed by keeping the coefficients j (computed by the analysis of the signal f) and cancelling all other coefficients for each scale. These coefficients constitute an approximation at the zero-scale of the projection of the signal f on the subspaces V_j.

The algorithm is divided into two steps. First, a mul-

Fig. 4. *Anadonta cygneae* (L.) surface. This range image is treated by keeping approximation at level 7.

tiresolution analysis according to Mallat's algorithm is performed in order to compute the approximate and detailed coefficients at level j: a^j and d^j. The reconstruction is then performed by only taking into account the coefficients (approximation or detail) corresponding to the explored scale. The result is a non-subsampled view of the approximation or detail signals at level j. Thus, the result of the reconstruction is computed by deleting the approximate coefficients at the coarsest scale, then the reconstructed approximation is $f-A_jf$. Since the projection operator is linear:

$$A_0(f - A_jf) = A_0f - A_0(A_jf). \tag{14}$$

Hence,

$$\begin{aligned} A_0(f - A_jf) &= A_jf + D_1f + D_2f + \ldots + D_jf - A_jf \\ A_0(f - A_jf) &= D_1f + D_2f + \ldots + D_jf. \end{aligned} \tag{15}$$

This approach is similar to the Daubechies' cascade algorithm, which is used in the reconstruction of scale and wavelet functions. If $f=\varphi_{j,0}$, then $a_n^j=\delta(n)$ and $d_n^j=0$, therefore the projection of $\varphi_{j,0}$ with the operator A_j is given by the formulae:

$$\begin{aligned} A_j\varphi_{j,0} &= \sum_{n=-\infty}^{+\infty} \langle \varphi_{j,0}, \varphi_{j,n} \rangle \varphi_{j,n} \\ A_j\varphi_{j,0} &= \sum_{n=-\infty}^{+\infty} \delta(n)\varphi_{j,n} \\ A_j\varphi_{j,0} &= \varphi_{j,0} \end{aligned} \tag{16}$$

and

$$A_0(A_j\varphi_{j,0}) = A_0\varphi_{j,0}. \tag{17}$$

This equation justifies the reconstruction of the scaling function $\varphi_{j,0}$ from a Dirac pulse and the details that have been erased. The same operation can be performed by considering $f=\psi_{j,0}$. In this case $a_n^j=0$ and $d_n^j=\delta(n)$, resulting in the following equation:

$$A_0(D_j\psi_{j,0}) = A_0\psi_{j,0}. \tag{18}$$

Thus, an approximation of the wavelet function can be obtained with any desired resolution.

4. Results: application to the range image of shell topography

Using the cascade algorithm, a multiresolution analysis has been performed on range images of

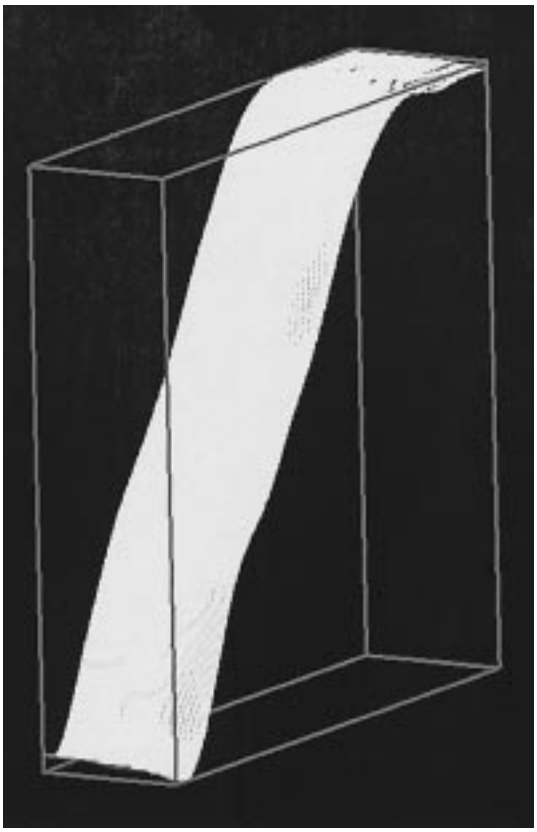

Fig. 5. 3D view of Fig. 4. At this scale, only general curvature of shell is visible. Height axis is exaggerated, the shell slope is not as steep as it appears.

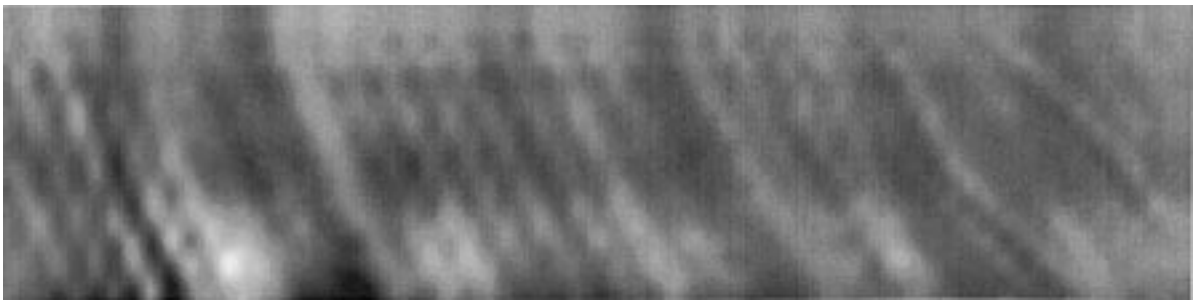

Fig. 6. *Anadonta cygneae* (L.) surface. In this example, range image is treated by keeping details at levels 5 and 4.

Anadonta cygneae (L.) shell topography. The bi-orthogonal basis is built with cubic B-splines (Vetterli and Kovacevic, 1995), which is a symmetrical function. The analysis is phase linear, as required for a priori isotropic image analysis. According to the multiresolution analysis described in the previous paragraph, two methods for extracting 3D features (i.e. growth increments) are proposed. The first method consists of extracting the object envelope, whereas the second extracts only details.

In order to extract the shell envelope, the approximation is made by deleting all the details after the analysis. The resulting information is viewed at the coarsest scale (Fig. 4 and in 3D Fig. 5). Although this image is not informative regarding the growth increments themselves, this peculiar appearance of the shell

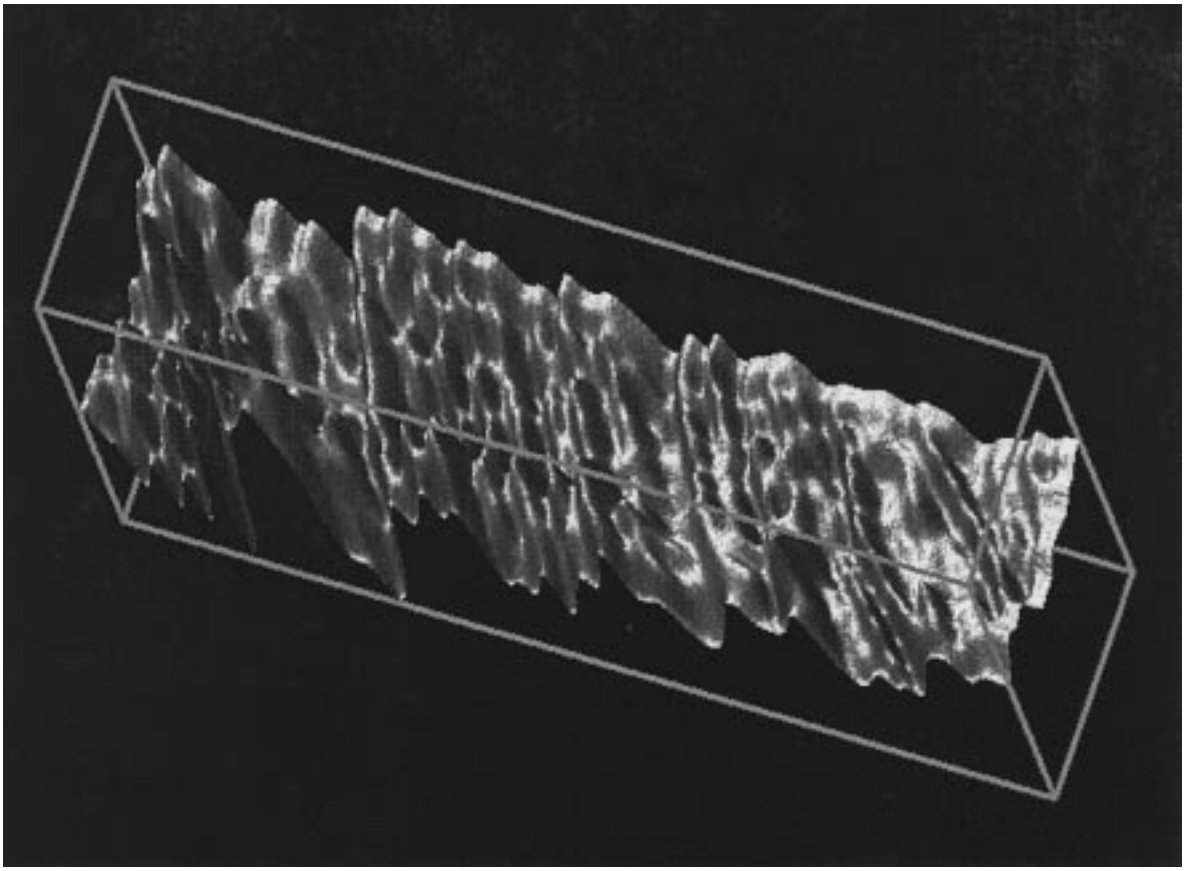

Fig. 7. 3D view of Fig. 6. By keeping details at levels 5 and 4, 4.2 to 2.8 mm growth increments are detected. They could correspond to seasonal and monthly increments.

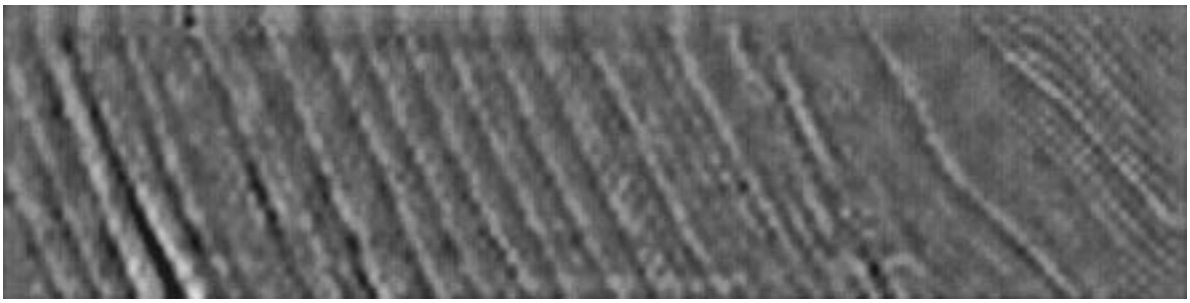

Fig. 8. *Anadonta cygneae* (L.) surface. In this example, range image is treated by keeping details at levels 4 and 3.

can be used for general shell curvature measurements, which can be critical for ontogenesis and species characterization.

The same kind of analysis can be achieved for each scale by deleting approximate coefficients and by keeping only detail coefficients, which are useful for growth increment measurement. For example, the range image given in Fig. 2 has been reconstructed after applying the algorithm at three different scales, using the following depth levels: 5 and 4 (Figs. 6 and 7), 4 and 3 (Figs. 8 and 9), 2 and 1 (Figs. 10 and 11). The first, second and third reconstructions show growth increments at various scales of resolution. The gap between increments and the amplitude of the crests decrease, as the resolution increases. The reconstruction allows a better representation of the growth increment signal. Using levels 5–4, 4–3 and 2–1, four main growth increments appear on average every 4.2 mm, 2.8 min, 800 μm, and 350 μm. The variations in absolute value of growth increment amplitude is not the subject of this paper. Further studies are in progress to characterize the difference in growth speeds of the various layers form-

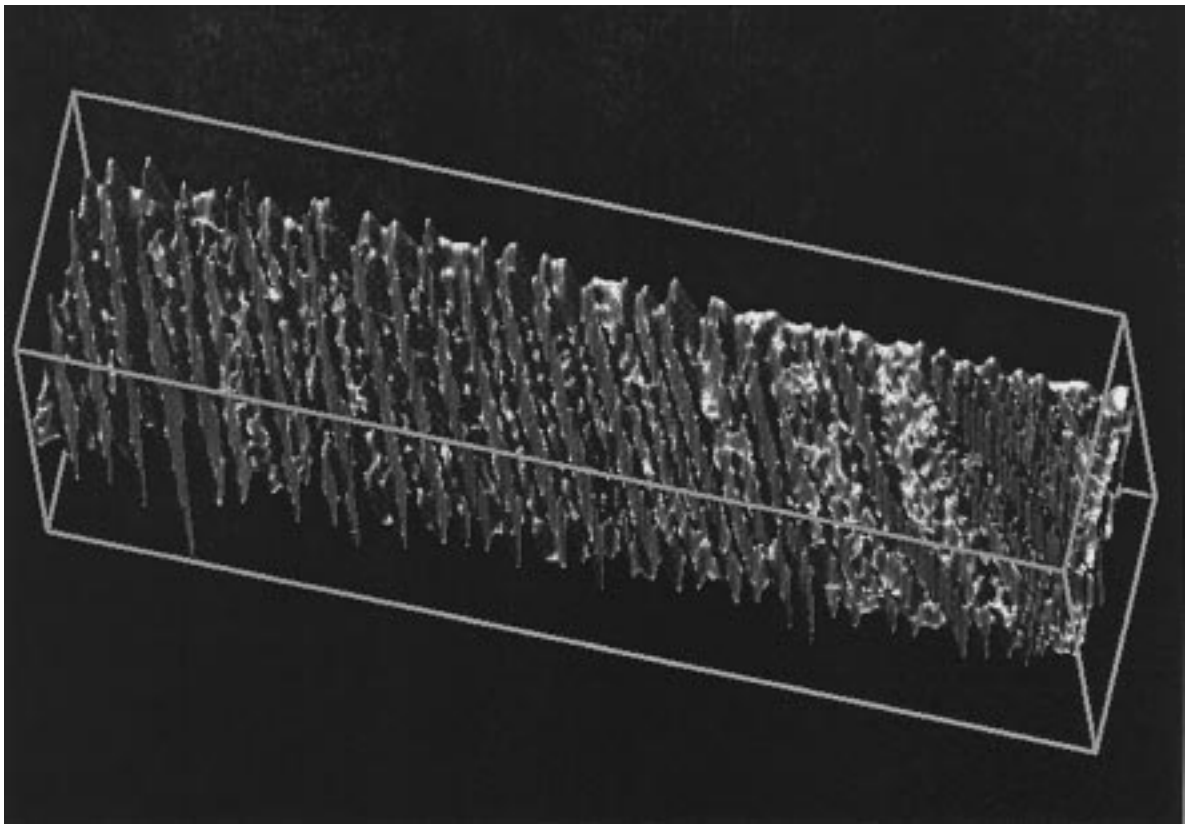

Fig. 9. 3D view of Fig. 8 treated by keeping details at level 4 and 3. Growth increments with smaller gap than in Fig. 7 are visible.

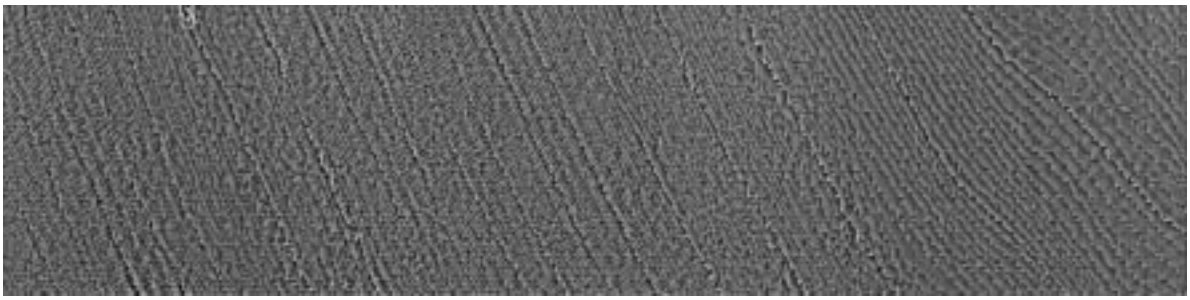

Fig. 10. *Anadonta cygneae* (L.) surface. In this example, range image is treated by keeping details at levels 2 and 1.

ing the shell, as well as their variation in chemical composition.

5. Conclusions

Multiresolution analysis with a bi-orthogonal cubic B-spline basis appears to be a powerful method for

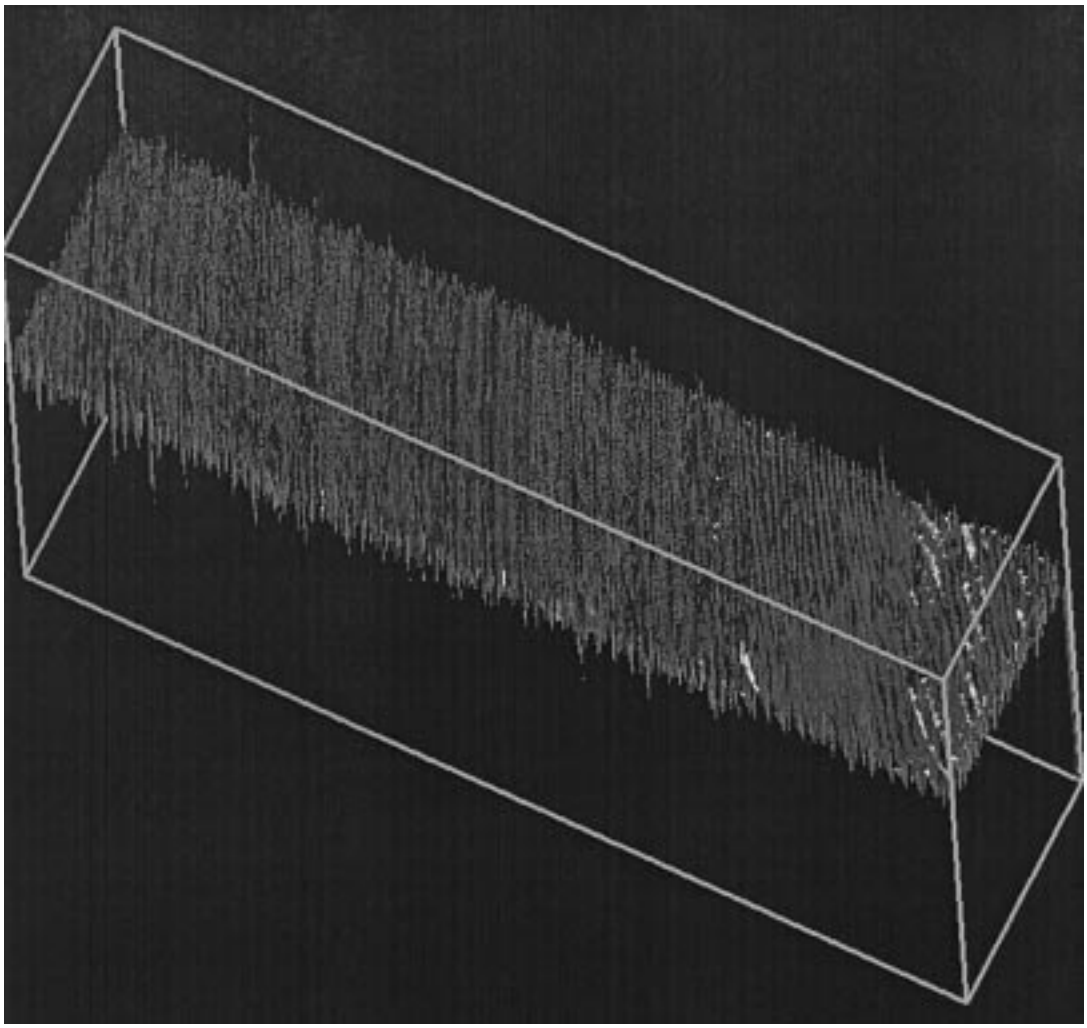

Fig. 11. 3D view of Fig. 10 treated by keeping details at levels 2 and 1. At these levels it seems likely that each growth increment is due to nyctemeral excretion.

extracting both spatial and frequency information from approximate and detail subspaces at various scales. This method has been applied to range images captured by a 3D laser scanning system and illustrated by the detection of growth increments on shell surface, to measure the various time lags involved in clam biomineralization. The multiscale representation created by the proposed method allows distinction between growth increments of various orders, which are related to bivalve ontogenesis and environmental stress. The algorithm used in this paper made it possible to obtain both detailed and approximate images at different scales, which have the same resolution as the initial image. The next step is the 3D representation of detailed information superimposed onto the object envelope in order to visualize in 3D the distance between ridges at various scales and still retaining the general shape of the shell. This method can equally be used to treat a virtual shell showing only the winter growth increments. Due to the high resolution of images, a mesh reduction algorithm can be used to simplify the object envelope while retaining the high resolution for the details. This method provides a description of the topography and a rapid model of the virtual shell.

Acknowledgements

This study was supported by a ''Fond Social Européen'' grant and the DOE's University Research Program in Robotics (Universities of Florida, Michigan, New Mexico, Tennessee and Texas, grant DOE-DE-FG02-86NE37968). This paper is a contribution to the theme ''Biogéochimie et diagenèse des carbonates de l'UM.R 5561 CNRS Biogéosciences-Dijon'' and to the ''Pôle Imagerie de l'Université de Bourgogne''. Two anonymous reviewers improved and clarified some points in the manuscript.

References

Clark, J., Zhang, G., Wallace, A.M., 1995. Image acquisition using fixed and variable triangulation. In: IEEE Fifth International Conference on Image processing, Edinburgh, Scotland, pp. 539–543.

Dolman, J., 1975. A technique for the extraction of environmental and geophysical information from growth records in invertebrates and stromatolites. In: Rosenberg, G.D., Runcorn, S.K. (Eds.), Growth Rhythms and the History of the Earth Rotation. John Wiley & Sons, London, pp. 191–221.

Fu, K.S., Gonzalez, R.C., Lee, C.S.G., 1987. Robotics: Control, Sensing, Vision and Intelligence. McGraw-Hill, New-York, p. 580.

Garcia, A., Truchetet, F., Lalignant, O., Dumont, C., Verrecchia, E.P., Abidi, M.A., 1998. Multiscale analysis of 3D surface image: application to clam shell characterization. In: Three-Dimensional Image Capture and Applications, SPIE EI'98 San Jose, No. 3313, pp. 126–133.

Jarvis, R.A., 1983. A perspective on range finding techniques for computer vision. IEEE Transactions Pattern Analysis and Machine Intelligence 2, 122–139.

Koike, H., 1980. Microstructure of the growth increment in the shell of *Meretrix lusoria*. In: Omori, M., Watabe, N. (Eds.), The Mechanisms of Biomineralization in Animals and Plants. Tokai University Press, Tokyo, pp. 93–98.

Laurin, L., Gaspard, D., 1987. Variations morphologiques et croissance du brachiopode abyssal *Macandrevia africana* Cooper. Oceanologica Acta 10 (4), 445–454.

Mallat, S., 1989a. Multiresolution approximations and wavelet orthonormal bases of L2(R). Transaction American Mathematical Society 315 (1), 69–87.

Mallat, S., 1989b. A theory for multiresolution signal decomposition: the wavelet representation. IEEE Pattern Analysis and Machine Intelligence 11 (7), 674–693.

Meyer, Y., 1990. Ondelettes et Opérateurs I-Ondelettes. Hermann, Paris, p. 232.

Rhoads, D.C., Pannella, G., 1970. The use of molluscan shell growth patterns in ecology and paleoecology. Lethaia 3, 143–161.

Rosenberg, G.D., 1975. A comment on terminology: the increment and the series. In: Rosenberg, G.D., Runcorn, S.K. (Eds.), Growth Rhythms and the History of the Earth's Rotation. John Wiley & Sons, London, pp. 1–8.

Vetterli, M., Kovacevic, J., 1995. Wavelets and Subband Coding. Prentice Hall, Englewood Cliffs, New Jersey, p. 488.

Wada, K., Fujinuki, T., 1976. Biomineralization in bivalve molluscs with emphasis on the chemical composition of the extrapallial fluid. In: Watabe, N., Wilbur, K.M. (Eds.), The Mechanisms of Mineralization in Invertebrates and Plants. University of South Carolina Press, Columbia, pp. 175–190.

Wilbur, K.M., Salenddin, A.S.M., 1983. Shell formation. In: Wilbur, K.M. (Ed.), The Mollusca, Vol. 4. Academic Press, New York, pp. 235–287.

3D Scanners Ltd.,1995. Technical literature, South Bank Technopark, London, UK. http:\\www.3dscanners.com, Replica 500, 25H.